

# RSC Advances



This is an *Accepted Manuscript*, which has been through the Royal Society of Chemistry peer review process and has been accepted for publication.

*Accepted Manuscripts* are published online shortly after acceptance, before technical editing, formatting and proof reading. Using this free service, authors can make their results available to the community, in citable form, before we publish the edited article. This *Accepted Manuscript* will be replaced by the edited, formatted and paginated article as soon as this is available.

You can find more information about *Accepted Manuscripts* in the [Information for Authors](#).

Please note that technical editing may introduce minor changes to the text and/or graphics, which may alter content. The journal's standard [Terms & Conditions](#) and the [Ethical guidelines](#) still apply. In no event shall the Royal Society of Chemistry be held responsible for any errors or omissions in this *Accepted Manuscript* or any consequences arising from the use of any information it contains.

Cite this: DOI: 10.1039/c0xx00000x

www.rsc.org/xxxxxx

ARTICLE TYPE

## Exploration of octahedrally shaped $\text{MnCo}_2\text{O}_4$ catalyst particles for visible light driven photo catalytic water splitting reaction

S. M. A. Shibli,\*<sup>a</sup> P. S. Arun<sup>a</sup>, Anupama V. Raj<sup>a</sup>*Received (in XXX, XXX) Xth XXXXXXXXX 20XX, Accepted Xth XXXXXXXXX 20XX*

DOI: 10.1039/b000000x

The  $\text{MnCo}_2\text{O}_4$  catalyst with a smooth octahedral geometry and a band gap of 2.1 eV was developed for visible light driven photo catalytic water splitting process by considering the crucial role of Co(III)OH centres in  $\text{Co}_3\text{O}_4$  catalyst, cobalt(II) oxide and  $\text{Mn}^{3+}$  centres in the most active  $\text{Mn}_2\text{O}_3$  catalyst towards photo catalytic water splitting process. The formation of the  $\text{MnCo}_2\text{O}_4$  catalyst was confirmed from the results of XRD, EDAX and XPS. The smooth octahedral geometry of most of the crystals synthesized was visualized from the FE-SEM analysis. The photo catalytic efficiency of the catalyst was analyzed with respect to time, presence of sacrificial agent (methanol) and in presence of direct sun light. The 0.08g of the catalyst produced about 33mL of gaseous products from 20mL of water after 95minutes of visible light irradiation ( $\lambda > 420\text{nm}$ ). The overall water splitting efficiency was increased in presence of small amount of methanol; hydrogen GC spectra revealed that the evolved hydrogen gas in presence of methanol was extra pure. The reusability analysis revealed that the synthesized catalyst could be reusable after the activation process, it might be due to the surface restructuring of the active centres of the catalyst during the continuous water splitting process. There was a slight decrease in the activity of the reused catalyst it is due to the decrease in concentration of the octahedrally shaped crystals as evidenced by FE-SEM analysis. These results revealed that the developed octahedrally shaped  $\text{MnCo}_2\text{O}_4$  catalyst will be an essential part of future generation visible light driven water splitting catalysts.

### Introduction

Cobalt and manganese based photo catalytic materials are emerged as efficient catalytic materials for water splitting reactions<sup>1,2</sup>. The manganese oxides are able to provide thermodynamic driving force required to split water over a wide pH range<sup>3</sup>. The photosynthetic systems also the manganese play key role in water oxidation; the crucial component present in such system is  $\text{Mn}_4\text{CaO}_5$ <sup>4</sup>. More over the  $\text{Mn}_2\text{O}_3$  is reported as the most active catalyst for the water splitting process<sup>5,6</sup>. The catalytic activity of manganese oxide catalyst significantly increased in the basic medium, it may be due to the higher stability of  $\text{Mn}^{3+}$  ions in the basic medium<sup>7</sup>. The presence of  $\text{Mn}^{3+}$  in the oxide surface is essential for water oxidation, the  $\text{Mn}^{3+}$  ion disproportionate in to  $\text{Mn}^{2+}$  and  $\text{Mn}^{4+}$  at acidic and neutral pH and catalytic water oxidation efficiency of  $\text{Mn}^{3+}$  ion get decreased<sup>7</sup>. Manganese oxides are incorporated with  $[\text{Ru}(\text{bpy})_3]^{3+}$  along with  $\text{H}_2\text{O}_2$  or Ozone, in order to get higher catalytic activity under neutral and weak acidic conditions<sup>8</sup>. Silica supported  $\text{MnO}_x$  activated with  $[\text{Ru}(\text{bpy})_3]^{3+}$  are also emerged as efficient catalysts for water oxidation catalysts<sup>9</sup>. The spinel  $\text{Co}_3\text{O}_4$  and micro structured cobalt oxide were also used for efficient water oxidation catalysts in presence of visible light, however the cobalt oxide catalysts were severely deactivate due to the formation of cobalt hydroxide precipitate<sup>10</sup>. This

deactivation process could be significantly reduced in Co and Mn based spinel catalysts due to the Co-Mn synergistic interaction<sup>11,12</sup> accordingly these systems emerged as effective visible light driven water splitting catalysts. More over the Time-resolved observations of water oxidation intermediates on a cobalt oxide catalyst revealed the crucial role of Co(III)OH centres in the  $\text{Co}_3\text{O}_4$  in determining the photo catalytic efficiency<sup>13</sup>. More over F. Song et al. recently explored a  $\text{Co}^{2+}$  and  $\text{Co}^{3+}$  containing mixed-valence catalyst for efficient visible light driven water oxidation<sup>14</sup>. In addition to that recently the cobalt(II) oxide nano particles are emerged as visible photo catalyst with higher efficiency<sup>15</sup>. These literature reports revealed that the Mn and Co based spinel catalyst with  $\text{Mn}^{3+}$  (the most active oxidation state of Mn for water splitting),  $\text{Co}^{2+}$  (cobalt(II) oxide) and  $\text{Co}^{3+}$  (active centre in spinel  $\text{Co}_3\text{O}_4$ ) with a band gap less than three will be an efficient catalyst for water splitting process under visible light. Salek et al.<sup>16</sup> reported that the  $\text{MnCo}_2\text{O}_4$ , with  $\text{Mn}^{3+}$ ,  $\text{Co}^{3+}$  and  $\text{Co}^{2+}$  ions at the octahedral and tetrahedral voids possess a visible light active band gap. More over J. Song et al. established the significance of shape selectivity in aerobic decontamination reactions<sup>17</sup>. In addition to this,  $\text{NiGa}_2\text{O}_4$  crystals with octahedral shape passed significantly higher photocatalytic water splitting efficiency compared to other geometries<sup>18</sup>. In this context development of  $\text{MnCo}_2\text{O}_4$  catalyst with octahedral shape, orbital and electronic characteristics for visible light driven photo catalytic water splitting is the objective

of the present study.

## Experimental materials and methods

### Synthesis procedure the $\text{MnCo}_2\text{O}_4$ catalyst

$\text{MnCl}_2 \cdot 4\text{H}_2\text{O}$ (AR) and  $\text{CoCl}_2 \cdot 6\text{H}_2\text{O}$ (AR) with a mole ratio 1:2 was taken and thoroughly mixed to a paste form. The paste form was added with excess water isopropanol (1:1) mixture, heated at  $100^\circ\text{C} \pm 3^\circ\text{C}$  with stirring, and evaporated to dryness. The mixture obtained was powdered and a small quantity of water isopropanol mixture added the same process was repeated. The mixture obtained was again powdered well and placed in a muffle furnace at  $470^\circ\text{C} \pm 5^\circ\text{C}$  for 12 hours. Every half an hour the mixture was carefully taken out, placed in air and stirred well. All the conditions were fixed based on reproducibility of the desired characteristics of the products, obtained after physico chemical analysis.

### Physicochemical characterization of $\text{MnCo}_2\text{O}_4$ catalyst

XRD patterns of the samples were recorded from a Bruker AXS D8 Advance Diffractometer using  $\text{Cu K}\alpha$  radiation. XRF analysis was carried out using a Bruker Model S4 Pioneer Sequential Wavelength Dispersive X-ray Spectrometer. XPS investigations were carried out on OMICRON EA-125 Photoelectron spectrometer at a base pressure better than  $\sim 1 \times 10^{-10}$  Torr. The Hitachi SU6600 Variable Pressure Field Emission Scanning Electron Microscope (FESEM) was used for obtaining FE-SEM images. Energy Dispersive Spectroscopic analysis was conducted using Horiba, EMAX (137eV). To examine the particle size distribution of the catalysts, transmission electron microscopy (TEM) (model TecnaiG2-20) was employed. A reference sample was analyzed and the accuracy was confirmed prior to the analysis of the actual sample, each time.

### Photo catalytic water splitting analysis of $\text{MnCo}_2\text{O}_4$ catalyst by using a photo reactor

The photo catalytic water splitting was investigated using photo reactor manufactured by Popular Science Apparatus Workshops Pvt. Ltd. (PSAW India) with visible light ( $\lambda > 420\text{nm}$ ) having 8 tubes of 8W(SANYO, Electric Co. Ltd. Japan) capacity, is concentrically arranged to get uniform illumination. 20mL distilled water was placed in a quartz tube containing appropriate amount of powdered  $\text{MnCo}_2\text{O}_4$  catalyst was irradiated with visible light for appropriate time with continuous stirring for photo catalytic water splitting. The gases evolved were collected by using a measuring gar. The 1mL methanol was used as the sacrificial agent. In that case the evolved gas was passed through saturated NaOH solution for the absorption of carbon dioxide gas. Direct sunlight was used to analyze the performance of the catalyst under sunlight and irradiation was performed on sunny days, from 12.30pm to 14.00pm (Kerala, India) when solar intensity fluctuations were minimum. The same experiments were repeated in 5days and average readings are included in the Figure 5C.

## Results and discussions

### Standardization of the synthetic parameters for $\text{MnCo}_2\text{O}_4$

The entire the synthetic parameters of the catalyst such as

precursors, solvent, temperature of evaporation and calcinations temperature were optimized based on the geometry, band gap, oxidation state of Mn and Co and the overall stability of the catalyst  $\text{MnCo}_2\text{O}_4$ . The catalyst was synthesized from chloride precursor for the preferred formation of smooth octahedral crystals with  $\text{Co}^{3+}/\text{Mn}^{3+}$  at octahedral site<sup>19</sup>. Kudo and Miseki<sup>20</sup> reported that a catalyst with smooth crystal structure will reduce the electron hole pair and resulted increased photo catalytic activity<sup>20</sup>. The standardized synthetic parameters for unsupported  $\text{MnCo}_2\text{O}_4$  catalyst were given in the experimental materials and methods. The physicochemical characterization of the  $\text{MnCo}_2\text{O}_4$  and extended assessment of its catalytic activity were carried out to fix the parameters based on reproducibility that was obtained with different batches of the synthesized products.

### Evidence for the formation of $\text{MnCo}_2\text{O}_4$

The nature of formation of the inverse spinel  $\text{MnCo}_2\text{O}_4$  catalyst was analyzed by comparing the XRD pattern of the synthesized  $\text{MnCo}_2\text{O}_4$  catalyst with available reports. The XRD pattern in Supporting Information (SI) Figure 1 revealed that no other phases except  $\text{MnCo}_2\text{O}_4$  spinel peaks were formed. The peaks were found to be sharp as Esko et al.<sup>21</sup> and Nissinen et al.<sup>22</sup> have also observed similar  $\text{MnCo}_2\text{O}_4$  inverse spinel phases at  $900^\circ\text{C}$ . The confirmation of the formation of inverse spinel  $\text{MnCo}_2\text{O}_4$  can be analyzed from binding energy spectra resulted from XPS analysis, the results were included below.

### Confirmation of the formation of $\text{MnCo}_2\text{O}_4$ catalyst

The binding energy spectrum shown in Figure 1 confirmed the formation of  $\text{Mn}^{3+}$ ,  $\text{Co}^{3+}$  and  $\text{Co}^{2+}$  in the synthesized catalyst. The  $\text{Mn}_{2p}$ -electron binding energy and  $\text{Co}_{2p}$  electron binding were measured using XPS. The spectrum consists of spin-orbit-split  $2p_{3/2}$  and  $2p_{1/2}$  peaks at about 641 and 653 eV respectively in the case of  $\text{Mn}(2p)$  is evidenced from the Figure 1B. These observations revealed the preferred formation of  $\text{Mn}^{3+}$  of  $\text{MnCo}_2\text{O}_4$  rather than  $\text{Mn}^{2+}/\text{Mn}^{4+}$  in  $\text{MnFe}_2\text{O}_4$ <sup>23,19</sup>. The peak at 780 eV (Figure 1A) reveals the presence of both  $\text{Co}^{3+}$  and  $\text{Co}^{2+}$  respectively for  $\text{Co}_{2p_{3/2}}$ <sup>23</sup>. The satellite peak at 786.4eV corresponds to  $\text{Co}^{2+}$  ion<sup>24</sup>. The peak at 795.2eV reveals  $\text{Co}_{2p_{1/2}}$  and the satellite peak at 803.6eV reveals the presence of  $\text{Co}^{3+}/\text{Co}^{2+}$  ion<sup>24</sup>. Zhang et al. have also reported about a similar XPS spectral pattern for  $\text{MnCo}_2\text{O}_4$  nanofibers<sup>25</sup>. These results together confirm the formation and existence of  $\text{MnCo}_2\text{O}_4$ .

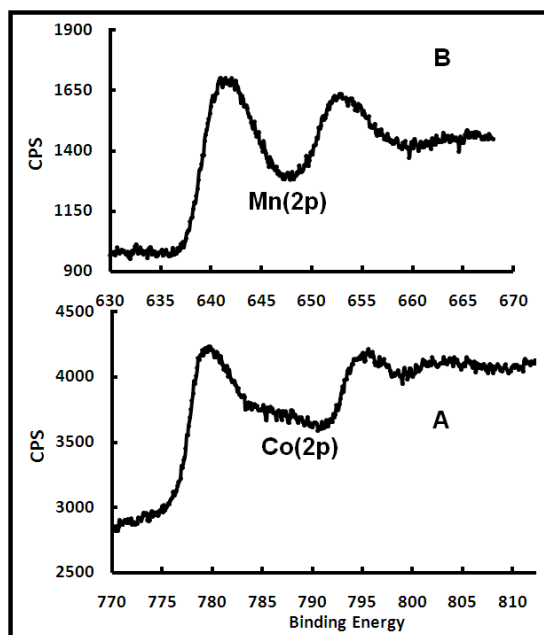


Fig. 1 XPS pattern of  $\text{MnCo}_2\text{O}_4$  confirmed the formation of  $\text{MnCo}_2\text{O}_4$  catalyst

#### Evidence for decreased recombination probability in terms of particle size

The distance that the photo generated electrons and holes have to migrate to the reaction sites on the surface of the catalyst become short when the particle size is very small and thus result in a decreased recombination probability<sup>20</sup>. Therefore the particle size of the catalyst was analyzed with TEM. The results of TEM analysis revealed that the synthesized particles possess an average particle size of 100nm as evidenced from the Figure 2. These results evidenced that the synthesized  $\text{MnCo}_2\text{O}_4$  catalyst particles have less size, hence it is predicted that the recombination possibility of electron hole pair is reduced and accordingly the catalyst will be efficient for photo catalytic water splitting reactions.

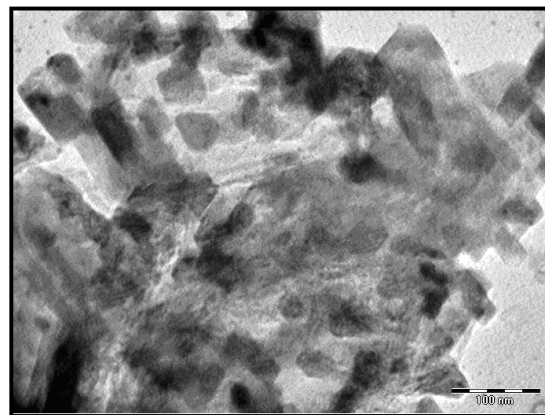


Fig. 2 TEM images of  $\text{MnCo}_2\text{O}_4$  evidenced the formation of nano particles of  $\text{MnCo}_2\text{O}_4$

#### Visualization of $\text{MnCo}_2\text{O}_4$ catalyst particles with octahedral morphological characteristics

The crystalline qualities of catalysts are vital for getting competent photo catalytic activity. The crystalline quality is higher, and then the number of defective sites will be less. The defective sites will act as trapping and recombination centres for photo generated electrons and holes, resulting in decreased catalytic activity<sup>20</sup>. The FE-SEM analysis was carried out to investigate the morphology of the synthesized catalyst particles of  $\text{MnCo}_2\text{O}_4$ . The FE-SEM images in the Figure 3(A1 to A4) revealed that the synthesized catalyst particles have smooth octahedral geometry with clearly seen crystal faces. Zhou et al. reported that in the case of  $\text{NiGa}_2\text{O}_4$  octahedron nanocrystals the electro hole recombination rate was lower compared to other shapes. Hence there will be an enhancement in photocatalytic activity<sup>18</sup>. The effectiveness of the synthetic procedure from chloride precursors resulted the smooth octahedral geometry of  $\text{MnCo}_2\text{O}_4$ <sup>19</sup>. The compositions of Mn and Co in the octahedrally shaped crystals were investigated using EDAX analysis. The results of EDAX analysis (SI Figure 4) revealed that the composition of all the crystals shown in the FE-SEM image Figure 3 was same and the Mn : Co ratio was 1:2.

Cite this: DOI: 10.1039/c0xx00000x

www.rsc.org/xxxxxx

ARTICLE TYPE

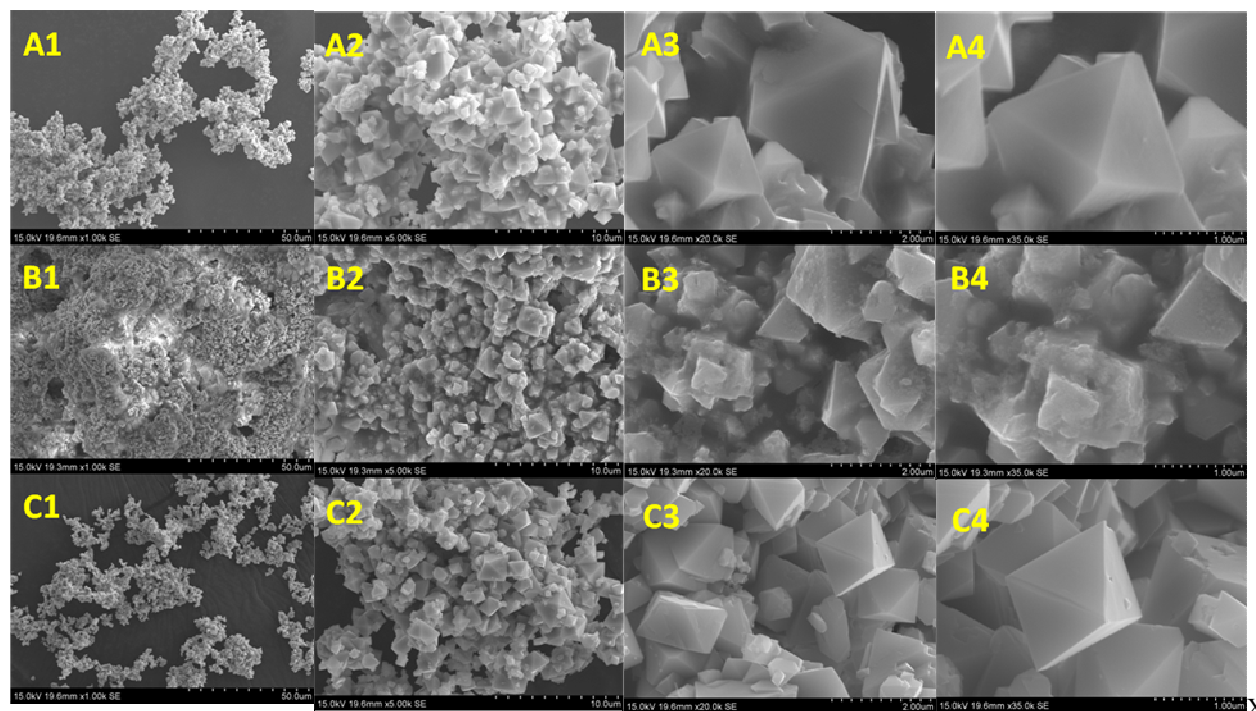


**Fig. 3** Visualization of octahedrally shaped particles in fresh  $\text{MnCo}_2\text{O}_4$  catalyst (A1 to A4), a surface restructured used  $\text{MnCo}_2\text{O}_4$  catalyst particles after drying (B1 to B4), and a decrease in concentration of octahedrally shaped particles in used catalyst after the activation process (C1 to C4).

### 5 Evidence for visible light driven photo catalytic activity of $\text{MnCo}_2\text{O}_4$ catalyst in terms of band gap

The band gap of a catalyst has a significant role in determining the photo catalytic water splitting efficiency, the band gap of the visible photo catalysts should be narrower than  $3\text{eV}$ <sup>20</sup>.  
10 Appropriate band tailoring is critical for the design of visible photo catalysts. The band gap of the synthesized  $\text{MnCo}_2\text{O}_4$  catalyst was evaluated by following the approach of Pankove and Lampert<sup>26</sup>, the Tauc plot and the uv-absorption spectrum (inset)

included in Figure 4. These results revealed that the  $\text{MnCo}_2\text{O}_4$  possess a band gap of 2.11eV similar to Salek et al.<sup>16</sup>.  $\text{MnCo}_2\text{O}_4$  is predicted as an effective catalyst for visible light driven photo catalytic water splitting process based on the results of TEM, FE-SEM and band gap analysis. The efficiency and practical feasibility of the synthesized  $\text{MnCo}_2\text{O}_4$  towards visible light  
20 driven photo catalytic water splitting process were analyzed in order to verify the prediction; the results were included in the next section.

Cite this: DOI: 10.1039/c0xx00000x

www.rsc.org/xxxxxx

ARTICLE TYPE

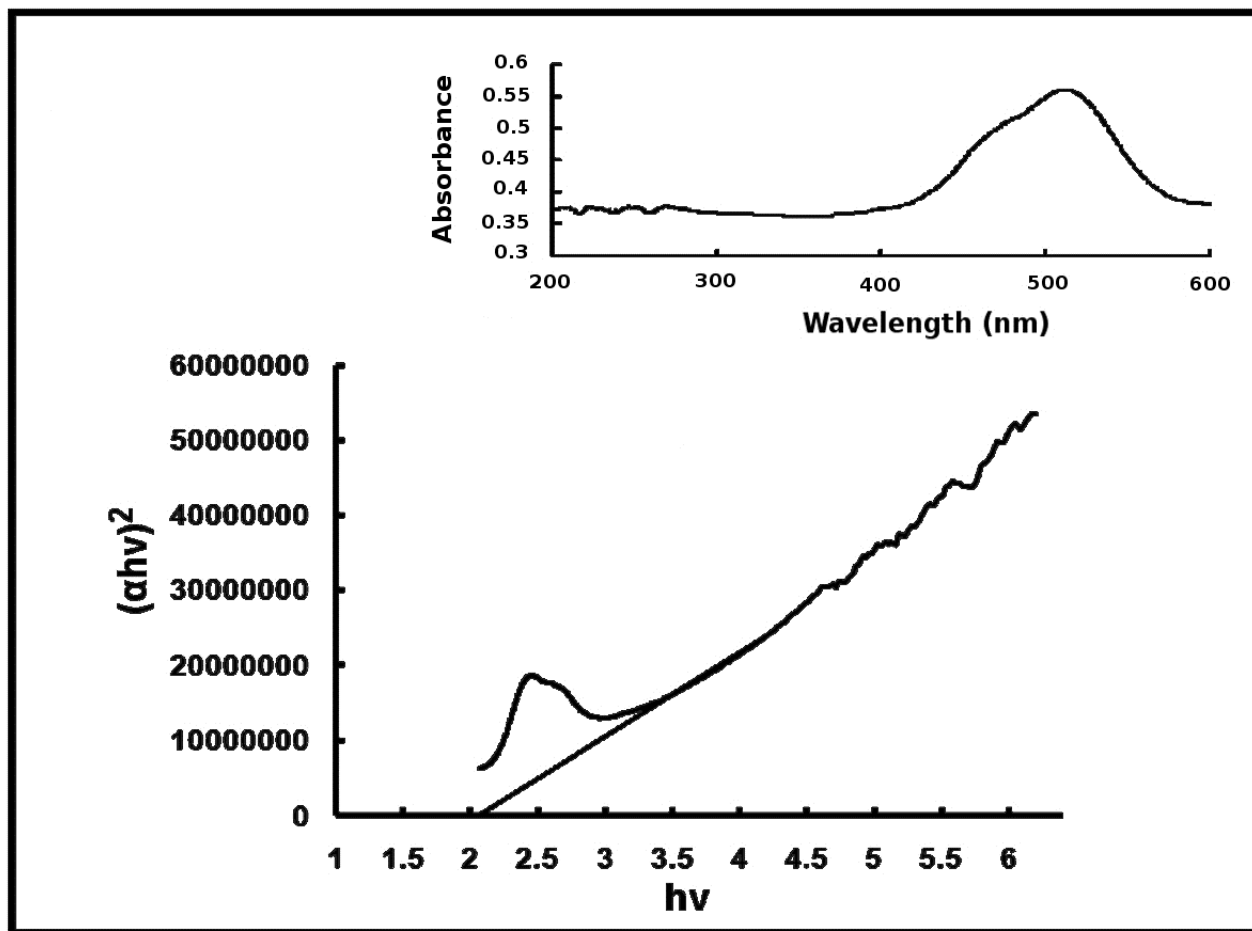


Fig. 4 UV-Visible absorption spectrum of  $\text{MnCo}_2\text{O}_4$  (inset) and corresponding Tauc plot used for calculating band gap of  $\text{MnCo}_2\text{O}_4$

#### Efficiency and practical feasibility of unsupported $\text{MnCo}_2\text{O}_4$ catalyst for photo catalytic water splitting in presence of visible light

##### Optimization of the amount of catalyst required for photo catalytic water splitting

The photo catalytic water splitting efficiency of different amount of the catalyst was analyzed for optimizing the amount of catalyst required for the water splitting process. The amount of the catalyst was increased from 0.01 to 1.5g for 20mL of water for 45 minutes of visible light irradiation ( $\lambda > 420\text{nm}$ ). As the amount of catalyst was increased from 0.01 to 0.08g the amount gas collected as a result of photo catalytic water splitting was also increased from 7.9mL to 22.6mL. When the amount of the catalyst was further increased from 0.08 to 1.5g there was no further significant increase in photo catalytic water splitting performance as evidenced from the S I Figure 2, hence 0.08g was fixed as the optimum amount for the water splitting reactions.

##### Evidence of excellent visible water splitting performance of unsupported $\text{MnCo}_2\text{O}_4$ catalyst (0.08g) as a function of time

The performance of the catalyst was monitored under visible light by means of a photo reactor manufactured by PSAW, Pvt. Ltd. India with visible light ( $\lambda > 420\text{nm}$ ) having 8 tubes each of 8W capacity, is concentrically arranged to get uniform illumination. The variation in photo catalytic water splitting performance in terms of volume of gas evolved (mixture of  $\text{H}_2$  and  $\text{O}_2$  in mL) with time was shown in Figure 5A. The effective water splitting process starts after 10 minutes of irradiation and the catalytic activity gradually increased and reached a maximum at 45 minutes as evidenced from the Figure 5A. The catalytic activity gradually decreased after 45 minutes however the catalyst was active after 95 minutes but the gaseous products liberated was significantly less compared to the initial amounts. The catalyst exhibited almost similar trend in presence of direct sunlight, but the catalyst retained its activity even after 120 minutes. The total gaseous products ( $\text{H}_2$  and  $\text{O}_2$ ) collected were about 36mL after 120 minutes from 0.08g of the catalyst as evidenced from Figure 5C. The gradual decrease in catalytic activity as evidenced from the Figure 5 might be due to the deactivation of the catalyst due

to surface restructuring of the Mn centres by the continuous water splitting reactions.<sup>9</sup> The most active type II heterostructured nano materials also still suffer from this type chemical instability, which significantly decreases the efficiency of the visible photo catalyst.<sup>27</sup> The FE-SEM images of the used catalyst shown in Figure 3(B1 to B4) also revealed that there was significant surface restructuring occurred on prolonged water splitting reactions.

Evidence for enhanced water splitting performance of unsupported  $\text{MnCo}_2\text{O}_4$  in presence of methanol

The sacrificial agents such as methanol act as hole scavenger and it enriches electrons in a photo catalyst and enhances photo catalytic hydrogen evolution reactions<sup>28</sup>. The effect of methanol on the water splitting behaviour of the  $\text{MnCo}_2\text{O}_4$  catalyst was

analyzed by adding 1mL methanol to 19mL of the distilled water before photo irradiation. The gas evolved during the photo catalytic water splitting process was passed through saturated NaOH solution for the absorption of  $\text{CO}_2$  released during the oxidation of methanol, getting pure hydrogen at the measuring chamber. The enhanced water splitting process in presence of methanol in terms of volume of gas collected ( $\text{H}_2$  gas in mL) was evidenced from the Figure 5B. The water splitting process started rapidly, increased to a maximum value at 50 minutes and gradually decreased. However the catalyst was effective even after 90 minutes but the activity was comparatively less. The hydrogen GC analysis revealed that the evolved hydrogen gas was pure, the GC spectra of evolved hydrogen is included in the SI Figure 3.

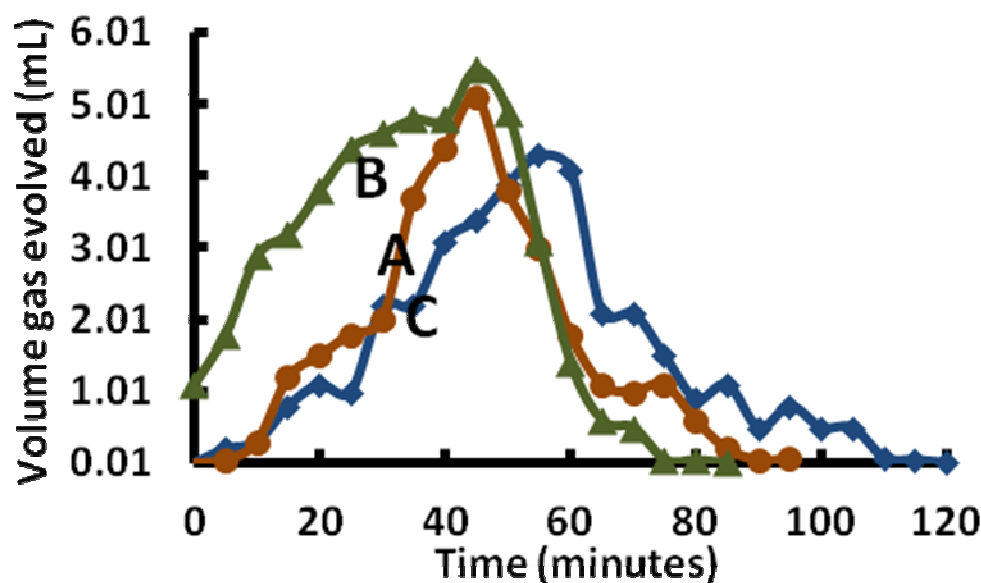


Fig. 5 Photo catalytic water splitting efficiency of 0.08g of  $\text{MnCo}_2\text{O}_4$  catalyst in presence visible light ( $\lambda > 420\text{nm}$ ) at room temperature with time (A), in presence of methanol (B) and in presence of sunlight (C)

#### Evidence for reusability of the catalyst

The used catalyst was again applied in the photo reactor for analyzing the reusability of the catalyst under visible light ( $\lambda > 420\text{nm}$ ) at room temperature for 45 minutes. The used catalyst was filtered, dried, activated at  $470^\circ\text{C} \pm 5^\circ\text{C}$  (muffle furnace) for 60 minutes and powdered for the reusability analysis. These parameters were fixed based on the activity, stability and life of the catalyst. The catalyst was active only after the activation process this confirmed the surface restructuring<sup>9</sup> of the catalyst that led the deactivation of the catalyst after the continuous water splitting process. The FE-SEM images shown in Figure 3(C1 to C4) of the catalyst after the activation process revealed that the extent of surface restructuring was lesser in the activated catalyst after the water splitting process. The activity of the reused catalyst with and without activation is shown in Figure 6. There was a slight decrease in the activity of used catalyst after the activation process it might be due to the decrease in concentration of octahedrally shaped crystals and slight surface restructuring as evidenced from the FE-SEM analysis shown in Figure 3(A2 to A4) and Figure 3(C2 to C4).

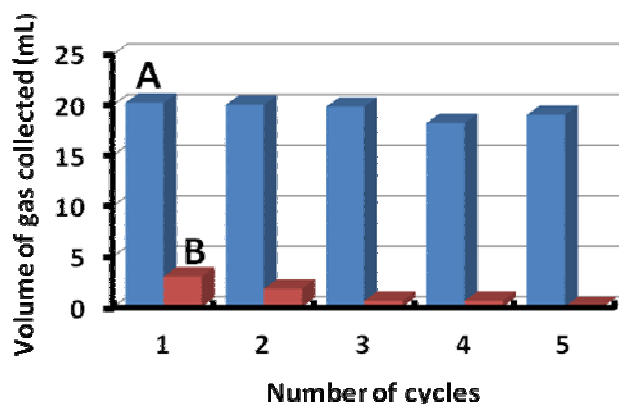


Fig. 6 Evidenced the reusability of  $\text{MnCo}_2\text{O}_4$  (A) with activation and (B) without activation

#### Predicted mechanism for overall performance of the catalyst

The octahedrally shaped  $\text{MnCo}_2\text{O}_4$  possesses a band gap of 2.11 eV, and hence it would generate electrons and holes necessary for the water splitting process in presence of visible light.<sup>20</sup> The enhanced activity of the catalyst without the presence of noble metal based co-catalyst/ sensitizer, might be due to the nano sized smooth octahedral crystal structure with the presence of active  $\text{Mn}^{3+}$ ,  $\text{Co}^{2+}/\text{Co}^{3+}$ . Moreover, there is a possibility of lesser electron hole recombination tendency of the octahedrally shaped crystals<sup>18</sup>. The decrease in activity of the catalyst after 45 minutes is attributed to the surface restructuring<sup>27</sup>, as evidenced from the FE-SEM Figure 3(B1 to B4) analysis. The higher activity of the reused catalyst after the activation process is due to the retention of the octahedral shape. However the slight decrease in the overall activity of the catalyst is due to the decrease in concentration of the octahedral crystals as evidenced from the FE-SEM Figure 3(C1 to C4) analysis.

## Conclusions

The  $\text{MnCo}_2\text{O}_4$  catalyst with a smooth octahedral geometry was tailored and synthesized by considering the crucial role of Co(III)OH centres in  $\text{Co}_3\text{O}_4$  catalyst, cobalt(II) oxide and  $\text{Mn}^{3+}$  centres in the most active  $\text{Mn}_2\text{O}_3$  catalyst towards photo catalytic water splitting process. The formation of the catalyst was confirmed from the results of EDAX, XRD and XPS analyses. The smooth octahedral geometry of the  $\text{MnCo}_2\text{O}_4$  catalyst was achieved from a chloride synthetic route and the resulted particles were visualized from FE-SEM images. More over the synthesized particles possess lesser size as evidenced from TEM. Hence the probability of recombination of electron hole pair was decreased. The band gap analyzes revealed that the synthesized  $\text{MnCo}_2\text{O}_4$  catalysts possess a band gap of 2.11eV, accordingly the catalyst was applied for visible light driven water splitting process. The 0.08g the catalyst produced about 33mL of gaseous products from 20mL of water after 95minutes of visible light irradiation ( $\lambda > 420\text{nm}$ ). The overall water splitting efficiency was increased in presence of small amount of methanol; hydrogen GC spectra revealed that the evolved hydrogen gas in presence of methanol was extra pure. The reusability analysis revealed that the synthesized catalyst could be reusable after the activation process, it might be due to the surface restructuring of the active centres of the catalyst during the continuous water splitting process.

## Acknowledgements

We thank M/s Sandhya Lekshmi, R. and Mr. Aravind Mohan, AgriInformatics, Indian Institute of Information Technology and Management-Kerala for designing the graphical abstract.

## Notes and references

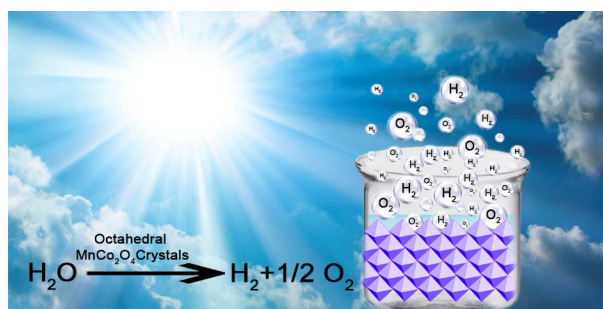
<sup>a</sup> Department of Chemistry, University of Kerala, Kariavattom Campus, Trivandrum, Kerala, India. Pin.695581 E-mail: [smashibli@yahoo.co.in](mailto:smashibli@yahoo.co.in)  
<sup>†</sup> Electronic Supplementary Information (ESI) available: [details of any supplementary information available should be included here]. See DOI: 10.1039/b000000x/

‡ Footnotes should appear here. These might include comments relevant to but not central to the matter under discussion, limited experimental and spectral data, and crystallographic data.

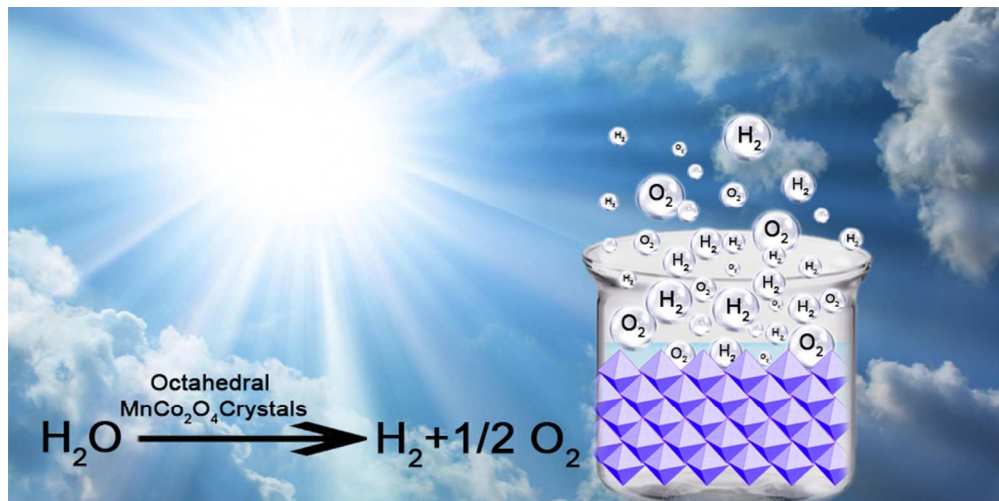
- Kanan, M. W., Nocera, D. G., In Situ Formation of an Oxygen-Evolving Catalyst in Neutral Water Containing Phosphate and  $\text{Co}^{2+}$ , *Science*, 321, 2008, 1072-1075.
- Listorti, A., Durrant, J., Barber, J., Artificial photosynthesis: Solar to fuel, *Nature Mater.*, 8, 2009, 929-930.
- Wiechen, M., Zaharieva, I., Dau, H., Kurz, P., Layered manganese oxide for water-oxidation: alkaline earth cations influence catalytic activity in a photosystem II-like fashion, *Chem. Sci.*, 3, 2012, 2330-2339.
- Sauer, K., Yachandra, V. K., A possible evolutionary origin for the Mn4 cluster of the photosynthetic water oxidation complex from natural  $\text{MnO}_2$  precipitates in the early ocean, *Proceedings of the National Academy of Sciences of the United States of America*, 99, 2002, 8631-8636.
- Morita, M., Iwakura, C., Tamura, H., The anodic characteristics of manganese dioxide electrodes prepared by thermal decomposition of manganese nitrate, *Electrochim. Acta*, 22, 1977, 325-328.
- Singh, A., Spiccia, L., Water oxidation catalysts based on abundant 1st row transition metals, *Coord. Chem. Rev.*, 257, 2013, 2607-2622.
- Takashima, T., Hashimoto, K., Nakamura, R., Mechanisms of pH-dependent activity for water oxidation to molecular oxygen by  $\text{MnO}_2$  electrocatalysts, *J. Am. Chem. Soc.*, 134, 2012, 1519-1527.
- Robinson, D. M., Go, Y. B., Greenblatt, M., Dismukes, G. C., Water Oxidation by  $\lambda\text{-MnO}_2$ : Catalysis by the Cubical  $\text{Mn}_4\text{O}_4$  Subcluster Obtained by Delithiation of Spinel  $\text{LiMn}_2\text{O}_4$ , *J. Am. Chem. Soc.*, 132, 2010, 11467-11469.
- Jiao, F., Frei, H., Nanostructured manganese oxide clusters supported on mesoporous silica as efficient oxygen-evolving catalysts, *Chem. Commun.*, 46, 2010, 2920-2922.
- Elizarova, G. L., Matvienko, L.G., Lozhkina, N.V., Parmon, V. N., Zamaraev, K. I., Homogeneous catalysts for dioxygen evolution from water. Water oxidation by trisbipyridylruthenium(III) in the presence of cobalt, iron and copper complexes, *React. Kinet. Catal. Lett.*, 16, 1981, 191-194.
- Okuno, Y., Yonemitsu, O., Chiba, Y., Manganese dioxide as specific redox catalyst in the photosensitized oxygen generation from water, *Chem. Lett.*, 12, 1983, 815-818.
- Conrad, F., Bauer, M., Sheptyakov, D., Weyeneth, S., Jaeger, D., Hametner, K., Car, P.-E., (...), Patzke, G. R., New spinel oxide catalysts for visible-light-driven water oxidation, *RSC Advances*, 2, 2012, 3076-3082.
- Zhang, M., Respinis, M. D., H. Frei, Time-resolved observations of water oxidation intermediates on a cobalt oxide nanoparticle catalyst, *Nature Chemistry*, 6, 2014, 362-367.
- Song, F., Ding, Y., Ma, B., Wang, C., Wang, Q., Du, X., Fu, S., Song, J., *Energy Environ. Sci.*, 6, 2013, 1170-1184.
- Liao, L., Zhang, Q., Su, Z., Zhao, Z., Wang, Y., Li, Y., Lu, X., Wei, D., Feng, G., Yu, Q., X., Cai, Zhao, J., Ren, Z., Fang, H., Hernandez, F. R., Baldelli, S., Bao, J., Efficient solar water-splitting using a nanocrystalline  $\text{CoO}$  photocatalyst, *Nature Nano Technology*, 9, 2014, 69-73.
- Salek, G., Fritsch, S. G., Dufour, P., Tenailleau, C., A simple preparation process of pure  $\text{Mn}_{3-x}\text{Co}_x\text{O}_4$  ( $x=1, 1.5, 2$ ) desert rose-like nanoparticles and their optical properties, *Int. J. Chem.*, 4, 2012, 44-53.
- Song J., Britt, D. K., Furukawa, H., Yaghi, O. M., Hardcastle, K. I., Hill, C. L., *J. Am. Chem. Soc.*, 133, 2011, 16839-16846.
- Zhou, S. X., Lv, X. J., Zhang C., Huang, X., Kang, L., Lin, Z. S., Chen, Y., Fu, W. F., *ChemPlusChem*, 79, 2014, 1-9.
- Wang, Y. W., Tian, W., Zhai, T., Zhi, C., Bando, Y., Golberg, D., Cobalt(II,III) oxide hollow structures: Fabrication, properties and applications, *J. Mater. Chem.*, 22, 2012, 23310-23326.
- Kudo, A., Miseki, Y., Heterogeneous photocatalyst materials for water splitting, *Chem. Soc. Rev.*, 38, 2009, 253-278.
- Esko, K. U., Rautama, E. L., Laitinen, M., Sajavaara, T., Karppinen, M., Control of oxygen nonstoichiometry and magnetic property of

- MnCo<sub>2</sub>O<sub>4</sub> thin films grown by atomic layer deposition, *Chem. Mater.*, 22, 2010, 6297–6300. 25
22. Nissinen, T., Valo, T., Gasik, M., Rantanen, J., Lampinen, M., *J. Power Sources*, 106, 2002, 109-115.
23. Kim, K. J., Heo, J. W., Electronic structures and optical properties of inverse spinel MnCo<sub>2</sub>O<sub>4</sub> thin films, *J. Korean Phys. Soc.*, 60, 2012, 1376-1380. 30
24. Sharma, Y., Sharma, N., Subba Rao, G.V., Chowdari, B.V.R., Studies on spinel cobaltites, FeCo<sub>2</sub>O<sub>4</sub> and MgCo<sub>2</sub>O<sub>4</sub> as anodes for Li-ion batteries, *Solid State Ionics*, 179, 2008, 587-597. 10
25. Zhang, Y., Luo, L., Zhang, Z., Ding, Y., Liu, S., Deng, D., Zhao, H., Chen, Y., *J. Mater. Chem. B*, 2014, 2, 529-535. 35
26. Pankove, J. I., Lampert, M. A., Model for electroluminescence in GaN, *Phys. Rev. Lett.*, 33, 1974, 361-365. 15
27. Wang, Y., Wang, Q., Zhan, X., Wang, F., Safdar, M., He, J., Visible light driven type II heterostructures and their enhanced photocatalysis properties: a review, *Nanoscale*, 5, 2013, 8326-8339. 40
28. Kawai, T., Sakata, T., Conversion of carbohydrate into hydrogen fuel by a photocatalytic process, *Nature*, 286, 1980, 474-476. 20

45



Graphical Abstract



80x39mm (300 x 300 DPI)